Ultrafast Electron Transfer in a Nanocavity. Dimethylaniline to Coumarin Dyes in Hydroxypropyl Gamma-Cyclodextrin

ARTICLE *in* THE JOURNAL OF PHYSICAL CHEMISTRY A · JANUARY 2007

Impact Factor: 2.69 · DOI: 10.1021/jp064412r · Source: PubMed

4 AUTHORS, INCLUDING:

Sudip Mondal
Visva Bharati University
35 PUBLICATIONS **851** CITATIONS

SEE PROFILE

Kankan Bhattacharyya
Indian Association for the Cultivation of Scie…
231 PUBLICATIONS **7,582** CITATIONS

SEE PROFILE

Ultrafast Electron Transfer in a Nanocavity. Dimethylaniline to Coumarin Dyes in Hydroxypropyl γ-Cyclodextrin

Subhadip Ghosh, Sudip Kumar Mondal, Kalyanasis Sahu, and Kankan Bhattacharyya*

Physical Chemistry Department, Indian Association for the Cultivation of Science, Jadavpur, Kolkata − 700 032, India

Received: July 13, 2006; In Final Form: September 1, 2006

Photoinduced electron transfer (PET) from *N*,*N*-dimethylaniline (DMA) to four coumarin dyes (C151, C481, C153, and C480) inside the cavity of hydroxypropyl γ-cyclodextrin (hpCD) is studied using femtosecond upconversion. The rate of PET is found to be nonexponential and to vary significantly with the coumarin dyes. The rate for C481 is 100 times faster than that for C480. The PET rate displays a bell-shaped dependence on the free energy change and thus reveals a Marcus-type inverted region. The anisotropy decay of the four dyes in hpCD are found to be very similar, and hence the observed variation in the rate of PET is not due to variation in rotational diffusion of the acceptors (coumarin dyes).

1. Introduction

Electron transfer (ET) in a confined region play a crucial role in many biological processes.[1,2] The classic Marcus model predicts a bell-shaped dependence of rate of ET on the free energy change. According to Marcus theory, the rate of electron transfer (k_{ET}) is given by[1,3]

$$k_{ET} = \frac{4\pi^2}{h} \frac{{V_{el}}^2}{\sqrt{2\pi\lambda_s k_B T}} \exp\left[-\frac{(\Delta G + \lambda)^2}{4\lambda k_B T}\right] \qquad (1)$$

where V_{el} is an electronic matrix element, ΔG is the free energy difference between the reactant and the product, $\lambda = \lambda_s + \lambda_I$, λ_S and λ_I, being the solvent and nuclear reorganization energy. For $-\Delta G < \lambda$, the rate of electron transfer (ET) increases with increase in $-\Delta G$. This is referred to as the normal region. However, for $-\Delta G > \lambda$ the rate of ET decreases with increase in $-\Delta G$. This is known as the Marcus inverted region.

An implicit assumption of the Marcus theory is that solvation is very fast, and at each point along the reaction coordinate the solvent reorganizes in a time scale faster than electron-transfer rate.[1,3−6] Zusman first considered the role of finite solvation time in electron transfer and showed that in the adiabatic limit, rate of ET is inversely proportional to the solvation time τ_L.[4a,c] Subsequently, several groups showed that electron transfer is strongly influenced by factors other than the solvent relaxation time. Ovchinnikova and later Zusman incorporated the role of fast classical vibrational modes in the stochastic electron transfer theory and used a coordinate-dependent sink.[4] This model is generally not valid in the inverted regime where ET is ultrafast and essentially irreversible. In a seminal paper, Sumi and Marcus introduced an irreversible stochastic model of ET with a wide sink term.[6] This led to the so-called 2D-ET model. This model involves a solvent polarization coordinate (X) and a low-frequency classical vibrational coordinate (Q). According to this model, the relaxation along Q is much faster than that along X and the effect of Q is included using a position dependent rate constant $k(X)$.[6]

Yoshihara and co-workers first reported that in neat donor (as solvent) photoinduced electron transfer (PET) displays a component faster than the solvation time.[7] Interestingly, even for ultrafast PET, the rate shows a bell-shaped dependence on ΔG and thus, a Marcus inverted region.[7] In order to explain the ultrafast ET process, Barbara and co-workers proposed a hybrid model which involves a classical low-frequency vibration, a classical solvent co-ordinate (X) and a high-frequency quantum mode.[8] Bagchi and co-workers developed a non-Markovian model and correlated the highly nonexponential ET process with the highly nonexponential solvation dynamics.[3] They noted that in most solvents, the solvation dynamics consist of an ultrafast subpicosecond inertial component and a slower component in tens of picoseconds. They showed that 30−40% of the solvent energy relaxation is sufficient to bring about ultrafast electron transfer.[3]

Recently, many groups have reported that solvation dynamics in nanoconfined systems exhibits a component which is slower by 2−3 orders of magnitude compared to that in bulk liquids.[9−15] It is obviously of interest to study how PET is influenced by the slow solvation dynamics and proximity of the donor and acceptor, in a nanocavity. Very recently, we have studied ultrafast ET from *N*,*N*-dimethylaniline (DMA) to four coumarin dyes of C151, C153, C480, and C481 (Scheme 1) in a micelle.[16] We found that the ultrafast ET in a micelle exhibits a Marcus inverted region. In the present study, we show that similar Marcus inverted region exists for ultrafast PET in the nanocavity of a cyclodextrin, hydroxypropyl γ-cyclodextrin (hpCD, Scheme 2A). We avoided γ-cyclodextrin because one of the coumarin dyes (C153) forms nanoaggregates in γ-cyclodextrin.[15]

2. Experimental Section

Laser grade coumarin dyes (C151, C481, C153, and C480) were purchased from Exciton Inc. and were used without further purification. Hydroxypropyl γ-cyclodextrin (hpCD, Aldrich) and *N*,*N*-dimethylaniline (DMA, Aldrich) were used as received. The steady-state absorption and emission spectra were recorded in a Shimadzu UV-2401 spectrophotometer and a Spex Fluoro-Max-3 spectrofluorometer respectively. The viscosity of the 50

* Corresponding author. E-mail: pckb@mahendra.iacs.res.in, Fax: +91-33-2473-2805.

10.1021/jp064412r CCC: $33.50
Published on Web 11/18/2006

SCHEME 1: Structures of Coumarin Dyes: (a) C153, (b) C480, (c) C151, and (d) C481

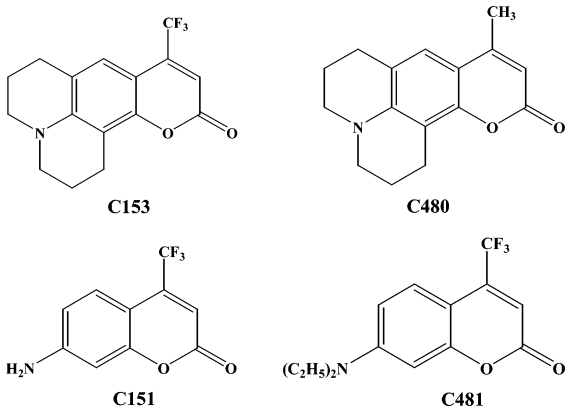

SCHEME 2: (A) Structure of Hydroxypropyl γ-CD and the (B) Coumarin−CD Complex

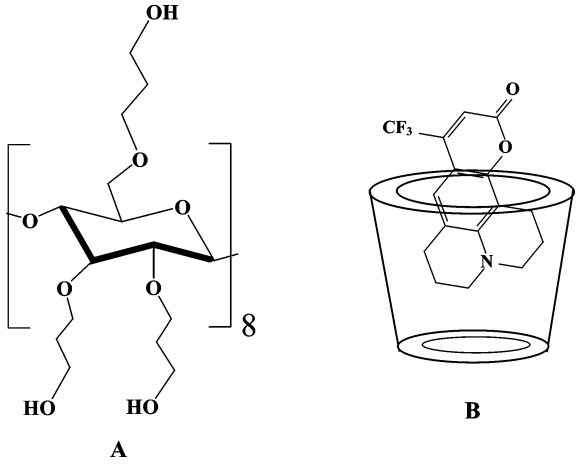

mM hpCD solutions was measured using a Ubblehode viscometer and found to be 1.15 mPaS at 25 °C.

In our femtosecond upconversion setup (FOG 100, CDP) the sample was excited at 405 nm using the second harmonic of a mode-locked Ti-sapphire laser (Tsunami, Spectra Physics) pumped by 5W Millennia (Spectra Physics). The fundamental beam was frequency doubled in a nonlinear crystal (1 mm BBO, $\theta = 25°$, $\phi = 90°$). The fluorescence emitted from the sample was upconverted in a nonlinear crystal (0.5 mm BBO, $\theta = 38°$, $\phi = 90°$) using a gate pulse of the fundamental beam. The upconverted light is dispersed in a monochromator and detected using photon counting electronics. A cross-correlation function obtained using the Raman scattering from ethanol displayed a full-width at half-maximum (fwhm) of the excitation pulse is 350 fs. The femtosecond fluorescence transients were fitted using a Gaussian shape for the excitation pulse.

To fit the femtosecond data, one needs to know the long decay components. These were detected using a picosecond set-up in which the samples were excited at 405 nm using a picosecond diode laser (IBH Nanoled-07) in an IBH Fluorocube apparatus. The emission was collected at a magic angle polarization using a Hamamatsu MCP photomultiplier (5000U-09). The time-correlated single photon counting (TCSPC) setup consists of an Ortec 9327 CFD and a Tennelec TC 863 TAC. The data is collected with a PCA3 card (Oxford) as a multichannel analyzer. The typical fwhm of the system response using a liquid scatterer is about 90 ps. The picosecond fluorescence decays were deconvoluted using IBH DAS6 software.

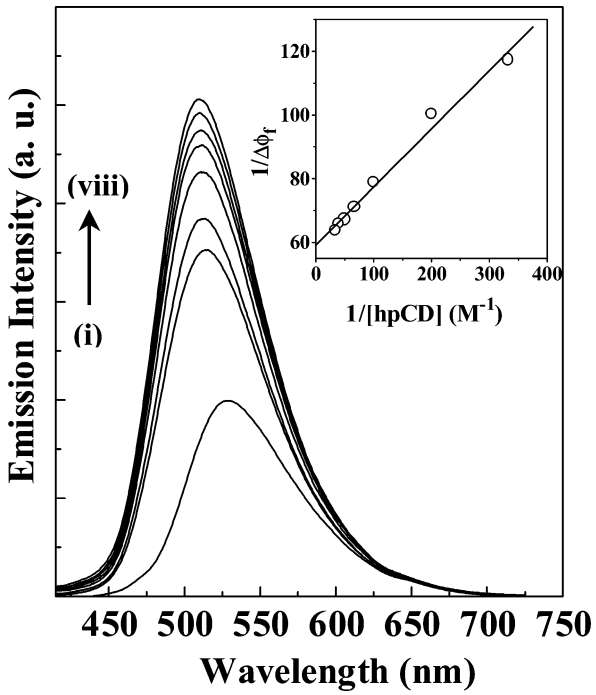

Figure 1. Emission spectra of C481 in (i−viii) 0−30 mM hpCD. The inset shows double reciprocal plot of $\Delta\phi_f$ vs concentration of hpCD.

The time-resolved emission spectra (TRES) are constructed using the steady-state emission intensity and the fluorescence decay parameters following the method of Maroncelli and Fleming.[21] The solvation dynamics is described by the decay of the solvent response function $C(t)$, defined by,[21]

$$C(t) = \frac{\nu(t) - \nu(\infty)}{\nu(0) - \nu(\infty)} \tag{2}$$

where $\nu(0)$, $\nu(t)$, and $\nu(\infty)$ are the emission frequencies at time zero, t, and infinity.

In order to study fluorescence anisotropy decay, the analyzer was rotated at regular intervals to get perpendicular ($I_\perp$) and parallel ($I_\parallel$) components. Then the anisotropy function, $r(t)$ was calculated using the formula

$$r(t) = \frac{I_\parallel(t) - GI_\perp(t)}{I_\parallel(t) + 2GI_\perp(t)} \tag{3}$$

The G value of the set-up was determined using a probe whose rotational relaxation is very fast, e.g., coumarin 153 in methanol, and the G value was found to be 1.5.

The oxidation and reduction potentials in a micelle exhibit a general shift from those in acetontrile.[19,20] hpCD contains eight glucose units linked by a ether linkage and is thus structurally similar to a poly oxyethelene surfactant, Triton X-100 (TX-100). Therefore, we used the reported reduction and oxidation potentials of coumarins and DMA reported in TX-100 micelle.[19a] In TX-100, the potentials differ by 0.13 V from those in acetonitrile.[19a] We have used this to calculate the reduction potential for C480 in hpCD.

3. Results

3.1. Binding of Coumarin Dyes to Hydroxypropyl γ-Cyclodextrin (hpCD). Figure 1 shows the effect of addition of hpCD on the emission spectrum of C481. In an aqueous solution, addition of 50 mM hpCD causes a blue shift of the emission maxima of the coumarin dyes along with an increase in

TABLE 1: Steady-State Emission Maxima and Binding Constant of Coumarin Dyes with hpCD

probe	λ_{em}^{max} in water (nm)	λ_{em}^{max} in 50 mM hpCD (nm)	binding constant, K_1 (M^{-1})	fraction bound in 50 mM hpCD
C151	494	485	75	0.80
C481	528	510	295	0.93
C153	549	535	300	0.93
C480	489	474	375	0.95

fluorescence intensity (Table 1). The emission maxima of C151, C481, C153, and C48D in hpCD are found to be at 485, 510, 535, and 474 nm, respectively (Table 1). Comparing these with the reported[22] emission maxima of the coumarin dyes in different solvents, it is inferred that the polarity inside the nanocavity of hpCD is lower than that in bulk water and close to that in alcohol.

If the stoichiometry of the coumarin dye (C):cyclodextrin (CD) (Scheme 2B) is 1:1, the equilibrium is given by

$$C + CD \overset{K_1}{\rightleftharpoons} [C:CD] \tag{4}$$

If ϕ_f and ϕ_0 denote the emission quantum yield of coumarins in the presence and in the absence of CD, $\Delta\phi_f$ ($= \phi_f - \phi_0$) is given by,[23]

$$\frac{1}{\Delta\phi_f} = \frac{1}{(\phi_\infty - \phi_0)} + \frac{1}{(\phi_\infty - \phi_0)\,K_1[CD]} \tag{5}$$

where, ϕ_∞ denotes the emission quantum yield of the coumarin dye when completely bound to hpCD. The value of K_1 was obtained from a double reciprocal plot of $\Delta\phi_f$ against [CD] (Figure 1, inset). The values of binding constant and fraction of the dyes bound to hpCD are given in Table 1. Obviously, almost all (~90%) of the coumarin dyes remain bound in the presence of 50 mM hpCD.

3.2. Binding of DMA with Coumarin:Cyclodextrin Complex and Quenching of Steady-State Emission. The absorption spectra of the coumarin dyes in hpCD remain unaffected on addition of DMA (Figure 2). This suggests that no complex involving the donor (DMA) and the acceptor (coumarins) is formed in the ground state of the coumarin dyes. On addition of DMA (electron donor) the emission intensity of the coumarin dyes inside the nanocavity decrease quite significantly while the emission maxima remain unaffected. The quenching of fluorescence intensity may be ascribed to electron transfer from DMA to the coumarin dyes. Figure 3 shows the effect of addition of DMA on the emission spectra of C481 in 50 mM

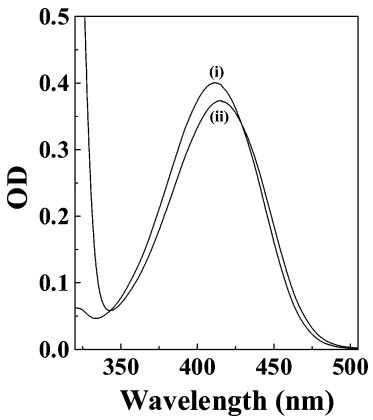

Figure 2. Absorption spectra of C481 in 50 mM hpCD in presence of (i) 0 mM and (ii) 15 mM DMA.

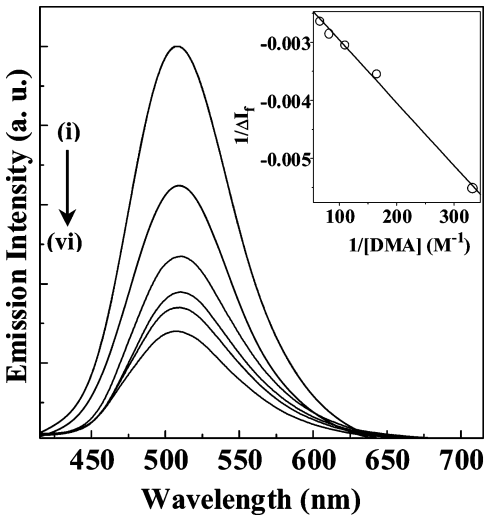

Figure 3. Emission spectra of C481 in 50 mM hpCD at DMA concentration of (i) 0 mM, (ii) 3 mM, (iii) 6 mM, (iv) 9 mM, (v) 12 mM, and (vi) 15 mM. The inset shows double reciprocal plot of ΔI_f vs DMA concentration.

hpCD. It is readily seen that addition of 15 mM DMA causes nearly 3.7 times decrease in the emission intensity of C481. Similar quenching was also observed for other coumarin dyes. In the case of C480, the extent of quenching is ~1.5 times.

The binding of DMA to the C481-hpCD complex corresponds to the following equilibrium,

$$[C:CD] + DMA \overset{K_2}{\rightleftharpoons} [C:CD:DMA] \tag{6}$$

The value of the binding constant, K_2 is obtained from the double reciprocal plot of ΔI_f against DMA concentration, where, $\Delta I_f = I_f - I_0$. I_0 and I_f are the emission intensities of C481 in 50 mM hpCD, respectively, in the absence and in the presence of DMA. The inset of Figure 3 shows such a plot for C481. The linearity of the plot indicates a simple 1:1:1 stoichiometry for the ternary complex coumarin−CD−DMA. The value of the binding constants is 175 M^{-1}. Thus, at 50 mM hpCD and 15 mM DMA, about 75% of the C481-hpCD complexes contain a bound DMA molecule.

In the absence of hpCD, effect of DMA is found to be far less efficient with much smaller quenching (~10%) of the emission intensity.

3.3. Time-Resolved Studies. Evidently, the DMA induced quenching should be accompanied by a shortening of fluorescence lifetime of the coumarin dyes. We, therefore, studied the fluorescence decays using a picosecond and a femtosecond set up.

3.3.1. Picosecond Studies of ET from DMA to Coumarin Dyes in the hpCD Cavity. Figure 4 shows the fluorescence decays of C481 and C480 in hpCD (recorded in a picosecond set-up) in 0 mM and 15 mM DMA. It is readily seen that for all the coumarin dyes the long component of decay remains almost unaffected on addition of DMA (Figure 4B). Also for C481, in hpCD the picosecond decays display no wavelength dependence in 15 mM DMA (Figure 4A). Thus, the picosecond decays do not explain the quenching of the emission intensity of coumarin dyes by DMA in the hpCD cavity. It seems that DMA affects the ultrafast part of the decay which is not resolved in a picosecond set-up (IRF ~90 ps). In the next section, using a femtosecond up-conversion set-up we show that addition of DMA markedly shortens the ultrafast part of the fluorescence decay.

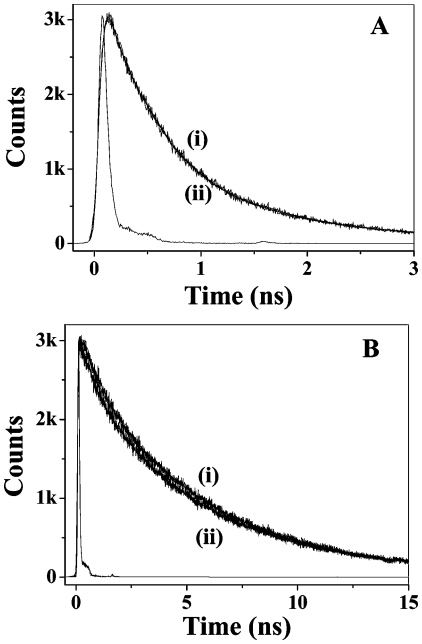

Figure 4. Picosecond transients of (A) C481 in 50 mM hpCD in the presence of 15 mM DMA at (i) $\lambda_{em} = 490$ nm and (ii) $\lambda_{em} = 550$ nm, and (B) C480 ($\lambda_{em} = 440$ nm) in 50 mM hpCD in the presence of (i) 0 mM and (ii) 15 mM DMA ($\lambda_{ex} = 405$ nm).

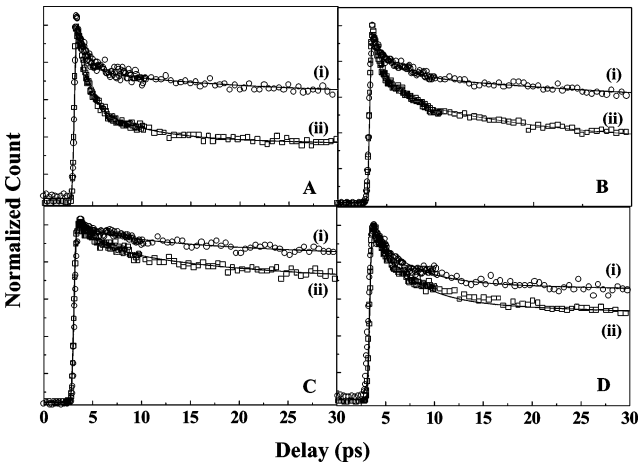

Figure 5. Femtosecond transients of (A) C151 ($\lambda_{em} = 450$ nm) and (B) C481 ($\lambda_{em} = 490$ nm) (C) C153 ($\lambda_{em} = 520$ nm) (D) C480 ($\lambda_{em} = 440$ nm) in 50 mM hpCD with DMA concentration (i) 0 mM and (ii) 15 mM ($\lambda_{ex} = 405$ nm).

3.3.2. Femtosecond Studies of ET from DMA to Coumarin Dyes in the hpCD Cavity. In order to study the effect of DMA on the ultrafast part of the fluorescence decays we recorded the decays using a femtosecond up-conversion set-up. Figure 5 shows the effect of addition of DMA on the ultrafast part of decay. It is readily seen that for C481 and C151 there is a significant change in the ultrafast initial part while the changes are smaller for C153 and C480 (Table 2).

It should be noted that for the coumarin dyes bound to hpCD, the fluorescence decays are wavelength dependent because of solvation dynamics. In the absence of DMA, for all the coumarin dyes at an emission wavelength at the red end of the emission spectrum, a rise precedes the decay. The rise originates from solvation dynamics. On addition of DMA the rise at the red end vanishes for C151 and C481 and its contribution for C153 is found to be very small. The absence of the rise component at the red end indicates that electron transfer is faster than solvation for these dyes in the hpCD cavity. Thus, the rise is masked by the ultrafast decay of the quenched emission of these three dyes.

TABLE 2: Fluorescence Decay Parameters of Coumarin Dyes in 50 mM hpCD in Water at 0 mM and 15 mM DMA Concentration

acceptor	λ_{em} (nm)	[DMA] (mM)	τ_1 (a_1)[a] (ps)	τ_2 (a_2)[a] (ps)	τ_3 (a_3)[a] (ps)
C151	450	0	1.1 (0.38)	130 (0.22)	4900 (0.4)
		15	1.6 (0.64)	100 (0.13)	4600 (0.23)
	520	0	1.2 (−0.29)	110 (−0.17)	5900 (1.46)
		15	4.6 (0.12)	95 (0.10)	5300 (0.78)
C481	490	0	3.4 (0.27)	150 (0.23)	800 (0.50)
		15	3.0 (0.53)	150 (0.29)	800 (0.18)
	550	0	1.5 (−0.30)	420 (0.71)	1500 (0.59)
		15	6.7 (0.21)	120 (0.28)	1550 (0.51)
C153	520	0	6.5 (0.11)	130 (0.18)	3300 (0.71)
		15	6.2 (0.26)	100 (0.07)	3100 (0.67)
	570	0	1.1 (−0.26)	900 (0.53)	3600 (0.73)
		15	0.8 (−0.10)	16 (0.14)	3440 (0.96)
C480	440	0	3.7 (0.34)	140 (0.17)	4900 (0.49)
		15	3.6 (0.45)	140 (0.27)	4850 (0.28)
	510	0	0.4 (−0.52)	5 (−0.33)	6480 (1.85)
		15	0.8 (−0.47)	130 (0.25)	5800 (0.78)

[a] ±10%.

In contrast to these three dyes, C480 continues to display a rise at the red end even in the presence of 15 mM DMA (Figure 6). This suggests that in the case of C480, ET is much slower, and in this case the slow component of solvation precedes ET. We studied solvation dynamics inside hpCD cavity in the presence of 0 and 15 mM DMA using C480 as a probe. The solvation dynamics in hpCD cavity is discussed in detail in the following section (3.4).

In order to determine the rate constant of the electron-transfer process (k_{ET}) we used the following equation

$$\frac{1}{\tau} = \frac{1}{\tau_0} + k_{ET} \tag{7}$$

where τ_0 and τ denote lifetime of the acceptor (coumarin), respectively 0 mM and 15 mM DMA. Except in the case of C480, we used the average lifetime of the fluorescence decay at the blue end in the absence and the presence of DMA, respectively, as τ_0 and τ. Since for C480 solvation is faster than ET, we used the long component of decay at the blue end. The

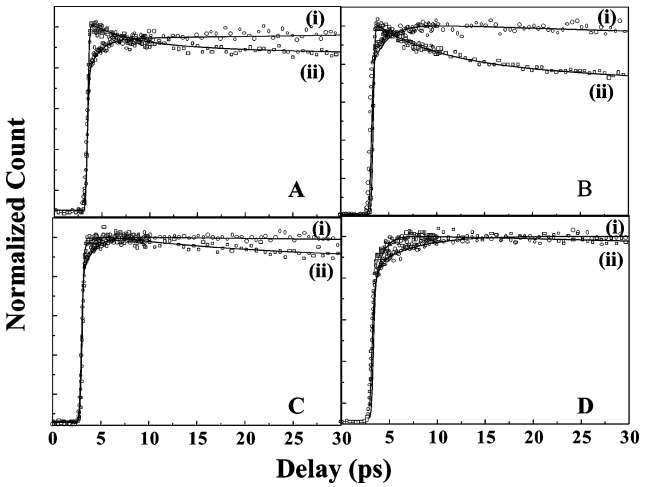

Figure 6. Femtosecond transients of (A) C151 ($\lambda_{em} = 520$ nm), (B) C481 ($\lambda_{em} = 550$ nm), (C) C153 ($\lambda_{em} = 570$ nm), and (D) C480 ($\lambda_{em} = 510$ nm) in 50 mM hpCD with DMA concentration (i) 0 mM and (ii) 15 mM ($\lambda_{ex} = 405$ nm).

TABLE 3: Electron-Transfer Parameters of Coumarin Dyes in 50 mM hpCD at 0 and 15 mM DMA Concentration

probe	[DMA], mM	ΔG (ev)	$<\tau>^a$ (ps)	k_{ET} (s^{-1})	$\ln(k_{ET})$
C151	0		4830		
	15	−0.82	4541	1.31×10^7	16.39
C481	0		747		
	15	−0.72	644	21.4×10^7	19.18
C153	0		3267		
	15	−0.50	3088	1.77×10^7	16.69
C480	0		4900[b]		
	15	−0.40	4850[b]	0.21×10^7	14.56

[a] $<\tau> = (\sum a_i\tau_i^2)/(\sum a_i\tau_i)$. [b] Longest component of decay.

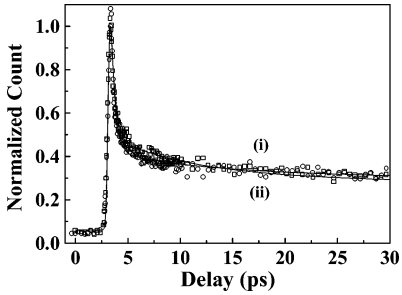

Figure 7. Femtosecond transients of C481 ($\lambda_{em} = 490$ nm) in bulk water with DMA concentration (i) 0 mM and (ii) 15 mM ($\lambda_{ex} = 405$ nm).

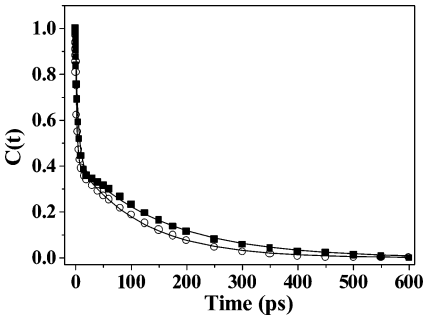

Figure 8. Decay of response function, C(t) of C480 in 50 mM hpCD with DMA concentration (a) 0 mM (○) and (b) 15 mM (■).

rate constants of ET for the different systems are listed in Table 3. As shown in Table 3, the rate constant of ET varies about 100 times from 21.4×10^7 s^{-1} for C481 to 0.21×10^7 s^{-1} for C480.

Figure 7 shows the ultrafast decay of C481 in bulk water in 0 and 5 mM DMA. Note, in bulk water, solubility of DMA is rather low (~5 mM) in the absence of hpCD. It is readily seen that the ultrafast portion of emission decays remains unaffected on addition of 5 mM DMA. This indicates that there is no ultrafast ET from DMA to coumarin dyes in bulk water. This may be ascribed to the relatively large donor−acceptor distance in bulk water. In contrast, inside the hpCD cavity the donor and the acceptor are held in close proximity leading to ultrafast ET.

3.4. Solvation Dynamics in hpCD in the Absence and Presence of DMA. Solvation dynamics inside the hpCD nanocavity was studied using C480 as a solvation probe. In the absence (as well as in the presence) of DMA, C480 exhibits emission wavelength-dependent decays and displays an ultrafast (~0.4 ps) and a comparatively slower (~5 ps) rise component at the red end (Table 2). Figure 8 shows decay of $C(t)$ for C480 in hpCD nanocavity in 0 and 15 mM DMA. In both the cases, the solvation dynamics exhibit two components: 3 ± 1 ps (~60%) and 140 ± 15 ps (~40%). This suggests that both in the presence and in the absence of DMA, there is a major component of solvation which is in a time scale <10 ps inside the hpCD cavity. Apparently, presence of one DMA molecule does not affect the solvation dynamics inside the CD cavity which already contains many water molecules.[9a] The ultrafast component of solvation obviously facilitates the ultrafast component of electron transfer which occurs in ≤10 ps time scale.

4. Discussion

The most important finding of this work is the ultrafast component of ET from DMA coumarin dyes inside the nanocavity of hpCD. It should be noted that in bulk water, addition of DMA causes negligible changes in the ultrafast component of decay of coumarin fluorescence (Figure 7), and hence there is no ultrafast component of ET. Obviously, the ultrafast ET in hpCD results from close proximity donor (DMA) and acceptor (coumarin dyes) in the same nanocavity of hpCD.

Another very interesting aspect of the present work is the marked variation of the rate of ET, depending on the acceptor. Several authors have considered the role of diffusion in ET.[17] The fluorescence anisotropy decay of all four coumarin dyes are very similar (Figure 9) with a single-exponential decay of time constant ~900 ps. The similarity in the anisotropy decays suggests that the variation of ultrafast ET inside the hpCD cavity is not due to variation in rotational diffusion. Note, the time constant of anisotropy decay (τ_R) is related to the hydrodynamic volume (V_h) as[24]

$$\tau_R = \frac{\eta V_h}{kT} \tag{8}$$

where η is the coefficient of viscosity and T is the temperature. From the time constant(τ_R), the hydrodynamic volume (V_h) is calculated to be 3220 Å.[3] The C:CD complexes is an ellipsoid with semiaxes a, b, c with volume $V_h = 4\pi abc/3$. For a and b, we used the reported width (9 Å) of hpCD.[25] Using this we calculated $c = 9.5$ Å. So that the length of hpCD complex is ~19 Å. The reported length of the hpCD is ~15 Å.[25] Thus, in a coumarin hpCD complex about 4 Å of the probe sticks outside the cavity.

Since in hpCD the ultrafast part of solvation is present even in the case of ultrafast ET, it is reasonable to expect a Marcus-like inverted region.[3−7] The spontaneity of the electron-transfer process from a ground state electron donor to an excited-state electron acceptor is determined by the standard free energy change (ΔG) of the PET reaction. In general, the ΔG for a photoinduced electron-transfer reaction between an electron donor (D) and an electron acceptor (A) is given by the Rehm−Weller equation.[26]

$$\Delta G = E(D/D^+) - E(C/C^-) - E_{00} - E_{IPS} \tag{9}$$

where E_{00} is the energy difference between S_0 and S_1 states of the electron-acceptor coumarin dyes. This is obtained from the wavelength at the intersection of the fluorescence and the excitation spectra. $E(D/D^+)$ and $E(C/C^-)$ denote the oxidation and reduction potentials of the electron donor (DMA) and electron-acceptor (coumarin dyes), respectively. The last term (E_{IPS}) of eq 9 denotes the ion pair stabilization energy in the medium and is given by[26]

$$E_{IPS} = \frac{e^2}{\epsilon_s r_0} \tag{10}$$

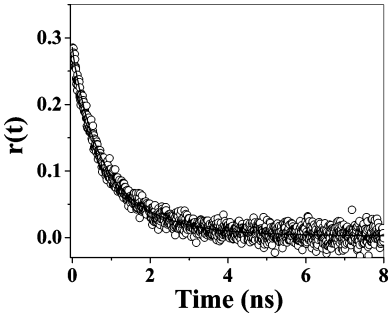

Figure 9. Fluorescence anisotropy decay (λ_{ex} = 405 nm) of C151 (λ_{em} = 450 nm) in 50 mM hpCD. The points denote the actual values of anisotropy, and the solid lines denote the best fit to the experimental data.

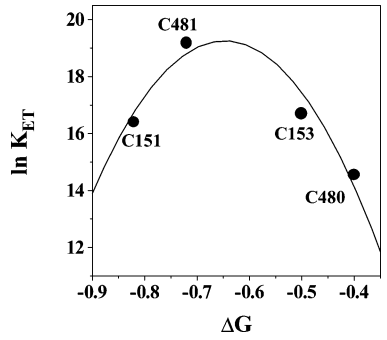

Figure 10. The ln(K_{ET}) vs ΔG plot for the coumarin−DMA system in 50 mM hpCD solution.

where, e is the electronic charge (= 1.602×10^{-19} C). The emission maximum of the coumarin dyes in hpCD are closed to that in methanol (ϵ_s = 32.7) or that in micelle (ϵ_s = 26).[19] Therefore, we used the $\epsilon_s \approx 30$ for hpCD. In eq 10, r_0 is the interaction distance between the donor and the acceptor. To calculate r_0, we have estimated the molecular volume (V) of the donor and the acceptor using a simple MM2 calculation. Assuming a spherical shape, we calculated the radius (r) of donor (and acceptor) from the relation, $r = (3V/4\pi)^{1/3}$. The sum of radii of the donor and the acceptor is r_0 and is found to be ~7 Å.[16] Similar values of the parameters are used earlier by other groups.[7,19,20] The ΔG values are listed in Table 3.

The ΔG dependence of rate PET for the four coumarin dyes in hpCD is shown in Figure 10. It is apparent that the plot of PET rate against ΔG (Figure 10) is bell-shaped and very clearly indicates a Marcus-type inverted region.

5. Conclusion

This work indicates that inside the nanocavity of hpCD, photoinduced ET (PET) from DMA to coumarin dyes exhibits a component in a few picosecond time scale. The rate of PET depends on the coumarin dyes. The rate of PET for C481 is 100 times faster than that for C480. For C481 and C151, PET is faster than solvation dynamics, and hence no rise is observed at the red end in presence of the quencher. For C480, even at the highest DMA concentration, solvation dynamics occur in 3 and 130 ps. The plot of the rate of ET vs ΔG shows a bell-shaped Marcus-type inverted region.

Acknowledgment. Thanks are due to Department of Science and Technology, India (Project Number: IR/I1/CF-01/2002), and Council of Scientific and Industrial Research (CSIR) for generous research grants. S.G., S.K.M., and K.S. thank CSIR for awarding fellowships. K.B. thanks Professor Biman Bagchi for many illuminating discussions.

References and Notes

(1) (a) Marcus, R. A. *Rev. Mod. Phys.* **1993**, *65*, 599. (b) Marcus, R. A. *Adv. Chem. Phys.* **1999**, *106*, 1.

(2) McArthur, E. A.; Eisenthal, K. B. *J. Am. Chem. Soc.* **2006**, *128*, 1068.

(3) (a) Bagchi, B.; Gayathri, N. *Adv. Chem. Phys.* **1999**, *107*, 1. (b) Gayathri, N.; Bagchi, B. *J. Phys. Chem.* **1996**, *100*, 3056. (c) Roy, S.; Bagchi, B. *J. Phys. Chem.* **1994**, *98*, 9207.

(4) (a) Zusman, L. D. *Chem. Phys.* **1980**, *49*, 295. (b) Ovchinnikova, M. Ya. *Teor. Eksp. Khim.* **1981**, *17*, 651. [*Theor. Exp. Chem.* **1982**, *17*, 507.] (c) Zusman, L. D. *Chem. Phys.* **1983**, *80*, 29.

(5) (a) Tavernier, H. L.; Barzykin, A. V.; Tachiya, M.; Fayer, M. D. *J. Phys. Chem. B* **1998**, *102*, 6078. (b) Barzykin, A. V.; Seki, K.; Tachiya, M. *J. Phys. Chem. A* **1999**, *103*, 9156. (c) Barzykin, A. V.; Frantsuzov, P. A. *J. Chem. Phys.* **2001**, *114*, 345.

(6) Sumi, H.; Marcus, R. A. *J. Chem. Phys.* **1986**, *84*, 4894.

(7) (a) Yoshihara, K. *Adv. Chem. Phys.* **1999**, *107*, 371. (b) Kobayashi, T.; Takagi, Y.; Kandori, H.; Kemnitz, K.; Yoshihara, K. *Chem. Phys. Lett.* **1991**, *180*, 416. (c) Pal, H.; Nagasawa, Y.; Tominaga, K.; Yoshihara, K. *J. Phys. Chem.* **1996**, *100*, 11964. (d) Shirota, H.; Pal, H.; Tominaga, K.; Yoshihara, K. *J. Phys. Chem. A* **1998**, *102*, 3089. (e) Shirota, H.; Pal, H.; Tominaga, K.; Yoshihara, K. *Chem. Phys.* **1998**, *236*, 355.

(8) (a) Barbara, P. F.; Olson, E. J. J. *Adv. Chem. Phys.* **1999**, *107*, 647. (b) Walker, G. C.; Akesson, E.; Johnson, A. E.; Levinger, N. E.; Barbara, P. F. *J. Phys. Chem.* **1992**, *96*, 3728. (c) Castner, E. W. Jr.; Kennedy, D.; Cave R. J. *J. Phys. Chem. A* **2000**, *104*, 2869.

(9) (a) Vajda, S.; Jimenez, R.; Rosenthal, S. J.; Fidler, V.; Fleming, G. R.; Castner, E. W. Jr.; *J. Chem. Soc. Faraday Trans.* **1995**, *91*, 867. (b) Nandi, N.; Bhattacharyya, K.; Bagchi, B. *Chem. Rev.* **2000**, *100*, 2013. (c) Bhattacharyya, K.; Bagchi, B. *J. Phys. Chem. A* **2000**, *104*, 10603. (d) Bhattacharyya, K. *Acc. Chem. Res.* **2003**, *36*, 95. (e) Pal, S. K.; Zewail, A. H. *Chem. Rev.* **2004**, *104*, 2099.

(10) Sen, P.; Roy, D.; Mondal, S. K.; Sahu, K.; Ghosh, S.; Bhattacharyya, K. *J. Phys. Chem. A* **2005**, *109*, 9716.

(11) (a) Nandi, N.; Bagchi, B. *J. Phys. Chem. B* **1997**, *101*, 10954. (b) Nandi, N.; Bagchi, B. *J. Phys. Chem.* **1996**, *100*, 13914.

(12) (a) Bandyopadhyay, S.; Chakraborty, S.; Balasubramanian, S.; Bagchi, B. *J. Am. Chem. Soc.* **2005**, *127*, 4071. (b) Faeder, J.; Albert, M. V.; Ladanyi, B. M. *Langmuir* **2003**, *19*, 2514. (c) Harpham, M. R.; Ladanyi, B. M.; Levinger, N. E. *J. Phys. Chem. B* **2005**, *109*, 16891. (d) Balasubramanian, S.; Pal, S.; Bagchi, B. *Phys. Rev. Lett.* **2002**, *89*, 115505−1. (e) Thompson, W. H. *J. Chem. Phys.* **2004**, *120*, 8125.

(13) (a) Frauchiger, L.; Shirota, H.; Uhrich, K. E.; Castner, E. W. Jr. *J. Phys. Chem. B* **2002**, *106*, 7463. (b) Grant, C. D.; Steege, K. E.; Bunagan, M. E.; Castner, E. W. Jr. *J. Phys. Chem. B* **2005**, *109*, 22273.

(14) (a) Riter, R. E; Undiks, E. P.; Kimmel, J. R.; Pant, D. D.; Levinger, N. E. *J. Phys. Chem. B* **1998**, *102*, 7931. (b) Shirota, H.; Horie, K. *J. Phys. Chem. B* **1999**, *103*, 1437. (c) Levinger, N. E. *Science* **2002**, *298*, 1722. (d) Riter, R. E.; Undiks, E. P.; Levinger, N. E. *J. Am. Chem. Soc.* **1998**, *120*, 6062. (e) Correa, N. M.; Levinger, N. E. *J. Phys. Chem. B* **2006**, *110*, 13050. (f) Yamauchi, A.; Amino, Y.; Shima, K; Suzuki, S.; Yamashita, T; Teramae, N. *J. Phys. Chem. B* **2006**, *110*, 3910. (g) Yamashita, T.; Amino, Y.; Yamauchi, A.; Teramae, N. *Chem. Lett.* **2005**, *34*, 988.

(15) Roy, D.; Mondal, S. K.; Sahu, K.; Ghosh, S.; Sen, P.; Bhattacharyya, K. *J. Phys. Chem. A* **2005**, *109*, 7359.

(16) Ghosh, S.; Sahu, K.; Mondal, S. K.; Sen, P.; Bhattacharyya, K. *J. Chem. Phys.* **2006**, *125*, 054509.

(17) (a) Saik, V. O.; Goun, A. A.; Nanda, J.; Shirota, K.; Tavernier, H. L.; Fayer, M. D. *J. Phys. Chem. A* **2004**, *108*, 6696. (b) Tavernier, H. L.; Laine, F.; Fayer, M. D. *J. Phys. Chem. A* **2001**, *105*, 8944. (c) Goun, A.; Glusac, K.; Fayer, M. D. *J. Chem. Phys.* **2006**, *124*, 084504.

(18) Pal, S. K.; Mandal, D.; Sukul, D.; Bhattacharyya, K. *Chem. Phys.* **1999**, *249*, 63.

(19) (a) Kumbhakar, M.; Nath, S.; Mukherjee, T.; Pal, H. *J. Chem. Phys.* **2004**, *120*, 2824. (b) Kumbhakar, M.; Nath, S.; Pal, H.; Sapre, A. V.; Mukherjee, T. *J. Chem. Phys.* **2003**, *119*, 388. (c) Kumbhakar, M.; Nath, S.; Mukherjee, T.; Pal, H. *J. Chem. Phys.* **2005**, *123*, 034705.

(20) Chakraborty, A.; Chakrabarty, D.; Hazra, P.; Seth, D.; Sarkar, N. *Chem. Phys. Lett.* **2003**, *382*, 508.

(21) Maroncelli, M.; Fleming, G. R. *J. Chem. Phys.* **1987**, *86*, 6221.

(22) Jones, G., II; Jackson, W. R.; Choi, C.-Y.; Bergmark, W. R. *J. Phys. Chem.* **1985**, *89*, 294.

(23) Wagner, B. D.; Stojanovic, N.; Day, A. I.; Blanch, R. J. *J. Phys. Chem. B* **2003**, *107*, 10741.

(24) (a) Balabai, N.; Linton, B.; Nappaer, A.; Priyadarshi, S.; Sukharevsy, A. P.; Waldeck, D. H. *J. Phys. Chem. B* **1998**, *102*, 9617. (b) Mondal, S. K.; Sahu, K.; Sen, P.; Roy, D.; Ghosh, S.; Bhattacharyya, K. *Chem. Phys. Lett.* **2005**, *412*, 228.

(25) Gaitano, G. G.; Brown, W.; Tardajos, G. J. *Phys. Chem. B* **1997**, *101*, 710.

(26) Rehm, D.; Weller, A. *Isr. J. Chem.* **1970**, *8*, 259.